# Impact of prospective climate change on water resources and crop yields in the Indrawati basin, Nepal

I. Palazzoli [a], S. Maskey [b], S. Uhlenbrook [b,c], E. Nana [a], D. Bocchiola [a,d,*]

[a] *Department ICA, Politecnico di Milano, L. Da Vinci, 32, 20133 Milano, Italy*
[b] *Department of Water Science and Engineering, UNESCO-IHE Institute of Water Education, Delft, The Netherlands*
[c] *Delft University of Technology, Water Resources Section, Delft, The Netherlands*
[d] *EVK2-CNR Association, San Bernardino 145, 24126 Bergamo, Italy*

Received 19 April 2014
Received in revised form 7 October 2014
Accepted 21 October 2014
Available online 26 November 2014

## 1. Introduction

Agriculture is heavily impacted by climate change, and yield reduction may result in the decline of *food security* worldwide, especially in mountainous areas (Bhatt et al., 2013; Malla, 2008; Olesen and Bindi, 2002; Parry et al., 2004). Agriculture requires much water for irrigation, and worldwide roughly 70% of the water is used by agriculture (Fader et al., 2011; Rost et al., 2008; *e.g.* Konar et al., 2011), and increasingly so under population growth pressure. Most relevant crops for food security are cereals, especially wheat, *Triticum* L., maize *Zea Mais* L, and rice *Oryza* L (Confalonieri et al., 2009; Supit et al., 2010; Torriani et al., 2007; Tubiello et al., 2000), requiring significant amounts of water for production, *i.e.* rainfall and often irrigation during summer or dry season (Bocchiola et al., 2013; Nana et al., 2014). Under climate change the need of water for cropping may increase, requiring adaptation strategies (*e.g.* Bocchiola et al., 2013; Torriani et al., 2007). Effects of climate on agriculture may include (i) effect of $CO_2$ increase on plant respiration cycle, especially for plants of type C3, and less for type C4 (Jarvis et al., 1999; Leuning, 1995; Morison, 1999), (ii) effects of temperature and rainfall changes (Brouwer, 1988), and (iii) effect of sea level rise, and reduction of cultivable lands (*e.g.* Zanoni and Duce, 2003). Climate change as projected for the 21st century may significantly alter crop production (FAO, 2009; Rosenzweig and Hillel, 1998). The recently issued assessment report 5 AR5 of the Intergovernmental Panel on Climate Change (IPCC) states that negative impacts of climate trends have been more common than positive ones worldwide (IPCC, 2013), and there are between 5 and 200 million additional people at risk of hunger within 2100 (Olesen and Bindi, 2002; Olesen et al., 2007).

This study focused on the Indrawati river basin, Nepal, Himalayas. Nepal's varied topography and social vulnerability make the country particularly susceptible to climate change (Agarwal et al., 2014; Awasthi et al., 2002; Eriksson et al., 2009; Karki and Gurung, 2012; Maskey et al., 2011; Nyaupanea and Chhetrib, 2009; Rai, 2007; Shrestha and Aryal, 2011). In turn, Nepal has low adaptive capac-ity to respond to the variability due to climate change (Dulal et al., 2010). Small scale (average 0.7 ha), subsistence agriculture is the mainstay of Nepal's economy, employing 78% of the workforce, and contributing nearly 36% of Nepal's GDP (World Bank, 2012). Only 27% of agricultural land has access to irrigation, and it is located above all in the Terai zone (the southern belt along the

* Corresponding author. Tel.: +390223996223; fax: +390223996207. *mail address:* daniele.bocchiola@polimi.it (D. Bocchiola).

Nepal–India boarder), whereas the great part of arable land is rainfed. The effect of recent climate change in Nepal includes rapid temperature increase (Eriksson et al., 2009; Malla, 2008; Rupa Kumar et al., 2006), erratic rainfall pattern, decreased length of Winter, and increased frequency and length of droughts (Sharma and Dahal, 2011). Therefore, the question arises whether present and perspective climate change may impact (negatively) on cropping, and food security locally. Even further, one needs a tool able to provide conjectures on future crop production, usable to develop (i) potential adaptation to climate change, (ii) modified cropping strategies including irrigation, and (iii) assessment and optimization of crop yield, and water usage under prospective climate change.

The objectives of this study were therefore (i) to set up a tool able to accurately mimic the hydrological cycle of the high altitude, topographically complex Indrawati river catchment, based upon climate inputs, (ii) to model accurately crop yield in the area for three key cereal species (wheat *Triticum* L., maize *Zea Mais* L., and rice *Oryza* L.), based upon little available agronomic information, and (iii) to investigate quantitatively the potential effect of prospective climate change scenarios (until 2100) on hydrology and crop production.

We used the Soil and Water Assessment Tool SWAT (Arnold et al., 2010) coupled with climate scenarios from 3 general circulation climate models (GCMs) included within the IPCC (Intergovernmental Panel for Climate Change) fifth assessment report 5AR, to obtain a range of hydrological and crop projections possibly providing a reference for initial assessment of future conditions in the area, and of potential adaptation strategies.

## 2. Material and methods

### 2.1. Description of study area

The Indrawati river basin (Fig. 1) extends from latitude 27°37′11″N to 28°10′12″N and longitude 85°45′21″E to 85°26′36″E, nested in the mid-hills of the central region of Nepal, and located about 50 km North-East of Kathmandu (capital city of Nepal). It is one of the seven sub basins of the larger Sapta Koshi basin.

The Indrawati river originates from the Himalayas (over 5850 meters above sea level [masl]), and flows southwards to meet the Sun Koshi River (at 623 masl), which then drains into the Sapta Koshi. Indrawati river is 59 km in length, and has a catchment area of 1228 km$^2$. The landscape is mostly made of rugged mountains, with occasional plateaus where farming is done, and covers a climatic range from subtropical to polar (Peel et al., 2007). Climate is governed by South Asian monsoon (carrying ca. 93% of total precipitation), and rainfall and snow melt are major sources of inflow. The rest of the year is considerably dry, with roughly 7% of the annual precipitation from November to April. Despite the little precipitation, Winter and Spring flow in the river are noticeable, due to snow melting. Temperatures range from 5 °C to 32.5 °C, and the

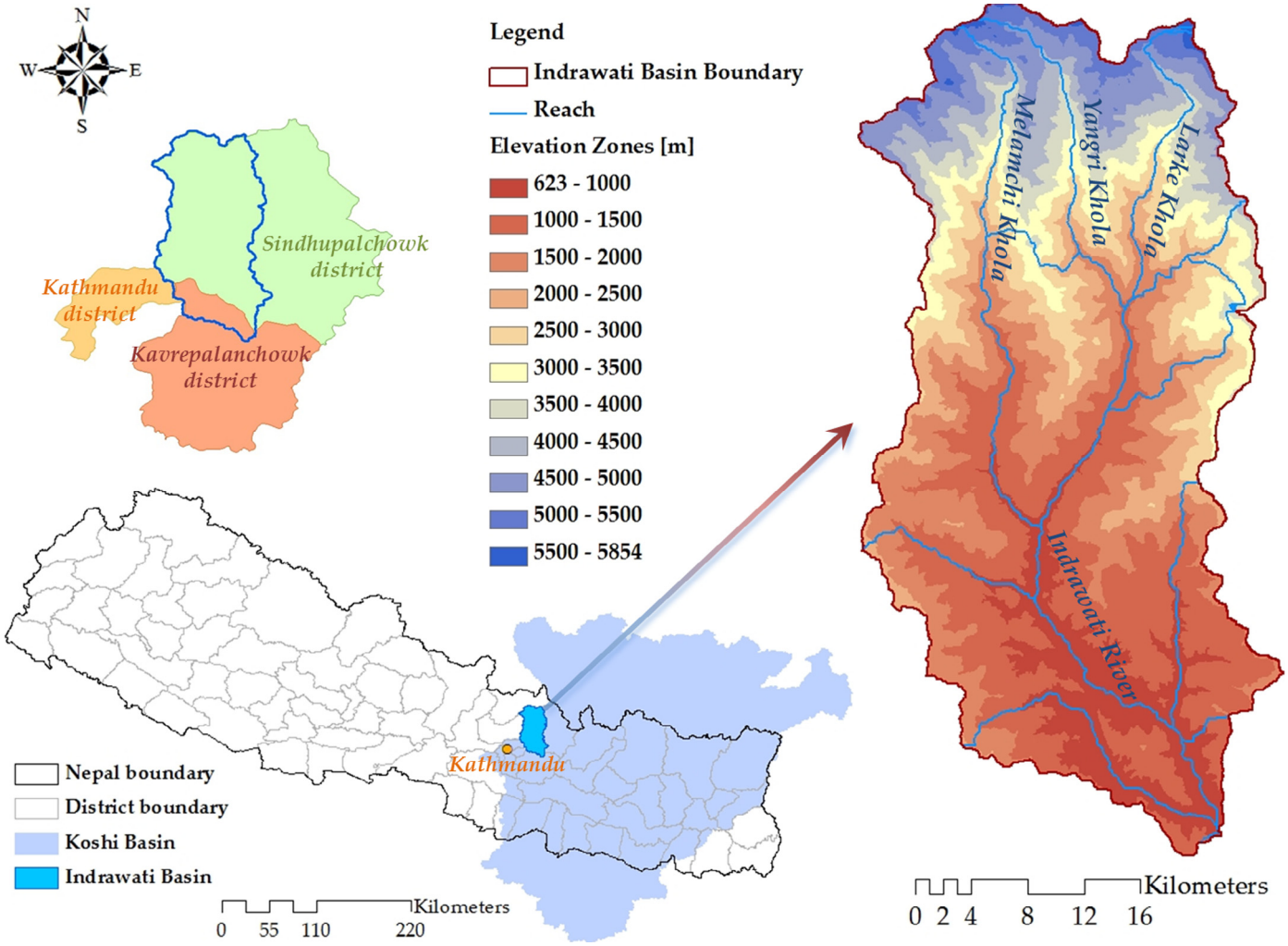


**Fig. 1.** Case study area. Indrawati basin location and elevation zones.

seasonal variation in temperature in the area is large (Bhattarai et al., 2002; Sharma, 2002). Agriculture covers about 400 km$^2$, approximately 50 km$^2$ of which has access to irrigation. Cereals like rice, wheat, maize and millet are predominant, with rice being the most preferred crop (monsoon rice in ca. 90% of cropping area, see also Bhatt et al., 2013). In the lowest areas (below 1200 masl) farmers grow three crops per year, including Spring paddy, due to access to year-round irrigation facilities in the river and tributaries, and warmer climate in the valleys. Farmers at the highest altitudes grow only two crops per year, even with irrigation, due to cooler temperatures. Farmers in the upper regions cannot grow Spring paddy, as it matures late due to the cool climate, which coincides with the plantation of the main season paddy.

Crop yield here is largely dependent on seasonal weather patterns (Bartlett et al., 2011; WWF, World Wildlife Fund, Nepal, 2012). According to recent findings (WWF, World Wildlife Fund, Nepal, 2012) in the Indrawati basin the water poverty index (WPI), measuring water resources availability (Cook et al., 2007) was estimated into 52.5 out of 100 (*i.e.* medium poor), with access to water being a major issue, due to the harsh topography and poor government planning. Therefore, the population of the area is at large risk of severe impacts from changes in temperature and precipitation patterns (Karki and Gurung, 2012; NAPA, 2010; WWF, World Wildlife Fund, Nepal, 2012).

### 2.2. Topography, land use and soil data

The SWAT model requires topographical (GIS input), hydrological, weather, and soil data. Topography was derived from a Digital Elevation Model (DEM) from the Shuttle Radar Topography Mission (SRTM, 2010), with resolution 90 m by 90 m (Fig. 1). Land use (Fig. 2a) was based on a 400 m resolution map by WaterBase projects of United Nations University (WaterBase, 2010). SWAT requires soil physio-chemical properties, namely hydrological group, texture, hydraulic conductivity, bulk density, and organic carbon content. The soil map of the catchment was derived from the Soil and Terrain (SOTER) database for Nepal (Dijkshoorn and Huting, 2009), based on ISRIC World Soil Information (Shakya, 2011).

### 2.3. Meteorological and hydrological data

The weather variables used in SWAT model are daily precipitation, maximum and minimum temperature, relative humidity, wind speed, and solar radiation. Weather data were collected from the Department of Hydrology and Meteorology of Nepal (DHM, 2010). Of the 13 weather stations (Fig. 2b) property of DHM in the study area, two are climatic stations (Panchkhal, station ID: 1036 and Nagarkot, station ID: 1043), measuring temperature, rainfall, and relative humidity, while the others only measure rainfall. Data from these stations cover the last 40 years, with some missing data (see Shakya, 2011). SWAT requires definition of temperature lapse rate within each sub watershed, to extrapolate temperature with altitude. Given the few temperature stations available, a standard temperature lapse rate (–6 °Ckm$^{-1}$) was taken, which was found acceptable, according to the hydrological model performance (Shakya, 2011). Using the available precipitation stations, an average lapse rate was found based upon yearly precipitation (2.5 mm km$^{-1}$ d$^{-1}$). SWAT model uses distributed precipitation from the measuring stations, extrapolated at different altitudes within each sub watershed using the lapse rate above. Solar radiation data were not available in this case. SWAT model estimates solar radiation within each subwatershed based upon topography, dates, and rainfall conditions (see Neitsch et al., 2011). While this may introduce some uncertainty, the lack of radiation data made use of SWAT estimates necessary. The SWAT model needs stream flow data for calibration and validation, made available here from DHM, at the Helambu station in Melamchi tributary outlet, and Dolalghat station at Indrawati basin outlet (Shakya, 2011).

### 2.4. SWAT model

The Soil-Water Assessment Tool (SWAT) (Arnold et al., 2012; Betrie et al., 2011; Schuol et al., 2008) is a watershed scale model developed by the United States Department of Agriculture-Agricultural Research Services (Neitsch et al., 2011). It is a physically based, semi-distributed model, running on daily time step. SWAT predicts water budget dynamics as well as crop yields in different Hydrological Response Units (HRUs) identified within the river basin. Each watershed is partitioned, according to the topography, into a number of sub-basins connected by a stream network (Fig. 2c). Each sub-basin is further divided into several homogeneous Hydrological Response Units (HRUs), *i.e.* lumped areas displaying unique land cover, soil, slope and management combinations. The plant growth component of SWAT is a simplified version of the Erosion Productivity Impact Calculator (EPIC; Izaurralde et al., 2006). In EPIC, plant development is based on accumulation of heat units, with potential biomass based on the method by Monteith and Moss (1977); a harvest index is used to calculate yield, and plant growth can be limited by temperature, water, nitrogen or phosphorus stress. The growth cycle of plants is regulated using heat unit theory, widely adopted in the present literature (*e.g.* Stöckle and Nelson, 1999; Stöckle et al., 2003). A plant will grow once a base temperature $T_b$ for growth is reached, and only the portion of the mean daily temperature exceeding $T_b$ will contribute to growth. Potential plant growth under ideal conditions of water and nutrients supply is calculated for each day of simulation, and actual growth is constrained by water and nutrient stress, and heat stress. Here, nutrient cycling was not considered for lack of data, and only water and temperature stress were accounted for. A total number of 12 sub-basins were identified for Indrawati catchment (Fig. 2c) and 572 HRUs were defined therein. Additional land use refinement was performed before applying thresholds and creating the HRUs. The agricultural land cover class *CRGI* (Cropland/Grassland mosaic + irrigated cropland and pasture) was split into four land cover classes (sub land uses), corresponding to different crops (Table 1).

For each type of crop, two management practices were specified, namely, planting operation and harvest and kill operation. All operations were scheduled by date (day and month) on the basis of the cropping calendar described by Bhattarai et al. (2002) and Sijapati et al. (2013). The basin was divided into 4 elevation zones, each one having a different growth period for each crop (Table 2). Subbasins from 1 to 3 were not considered as potential cropping areas, due to their average altitude around 4000 masl, much higher than the feasible crop cultivation range in Nepal. Spring rice was not cultivated in basins 4, 5, 6 and 7 (above 1200 masl), because Spring temperature is too low. Only rain-fed agriculture was considered, given scarce irrigation cover as reported, and it was assumed that only the land with slope <50% was cultivated.

In addition to scheduling of planting and harvest operation, the total number of heat units required for a plant to reach maturity was calculated for every crop, using the mean temperature within each subbasin. Each degree (°C) of the mean daily temperature above the base temperature of the crop was taken as one heat unit, as

$$PHU = \sum_{d=1}^{m} HU \tag{1}$$

where *PHU* gives the total heat units for crop maturity, *HU* is the number of heat units accumulated on day $d$, with $d = 1$ sowing date, and $d = m$ day of crop maturity. Harvest was carried out at crop maturity, and $m$ was taken as the number of days between planting and harvest.

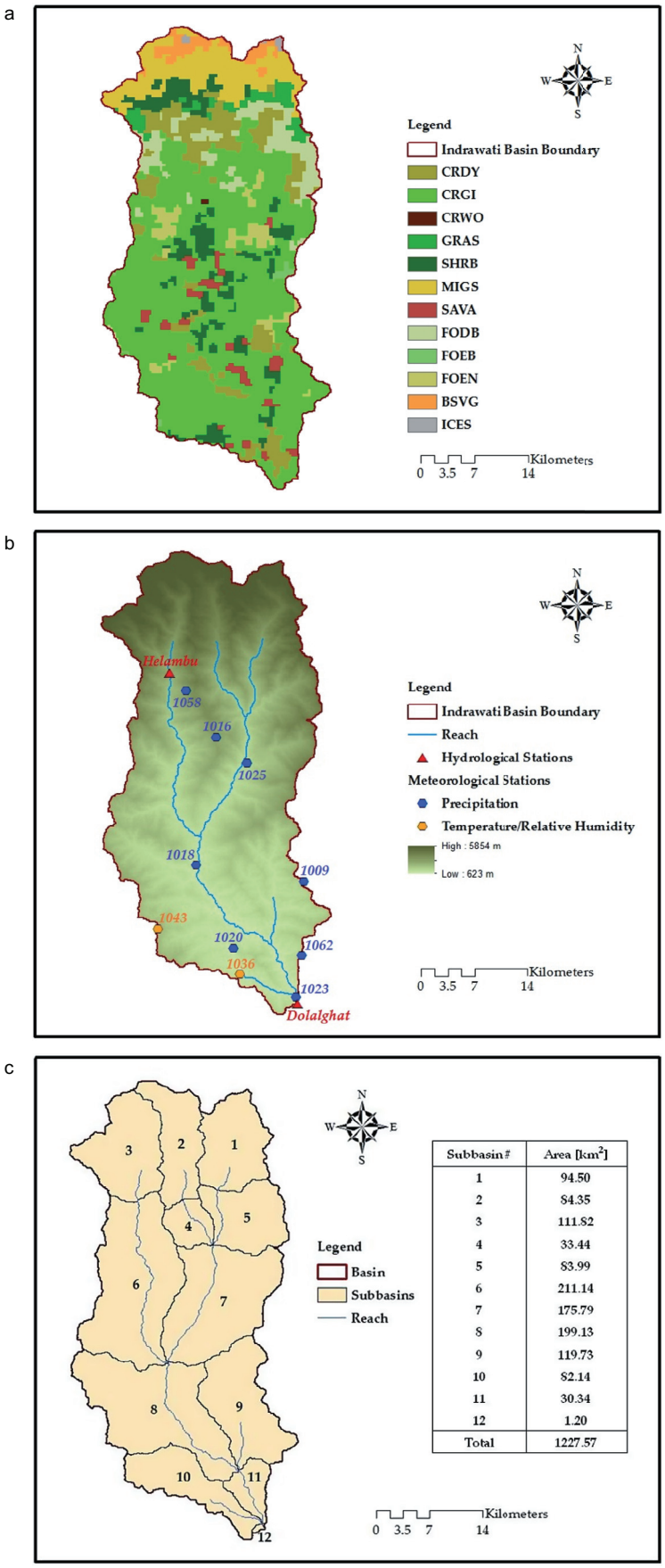


**Fig. 2.** SWAT model input. (a) Land use. CRGI, Cropland/Grassland mosaic + Irrigated cropland and pasture is the cropping area used here. (b) Meteorological and hydrological stations. (c) Subbasins partition.

**Table 1**
Indrawati basin. Subdivision of land use in class *CRGI* (Cropland/Grassland mosaic + Irrigated cropland and pasture).

| Sub land use | CRGI area [%] | Watershed area [%] |
|---|---|---|
| Rice | 22 | 12.3 |
| Maize | 25 | 13.9 |
| Winter wheat | 14 | 7.8 |
| Alfalfa | 39 | 21.7 |

Manual calibration of the hydrological module was pursued by trial-and-error approach, modifying the most important parameters as highlighted in a former sensitivity analysis (Shakya, 2011). Stream flow data from two gauges were used for hydrological calibration, one located at the Melamchi outlet in Helambu, and another one located at the basin outlet at Dolalaghat station (Fig. 2b), available daily (from 2001 to 2008) and monthly (1975 to 1990). Validation was carried out using daily stream flows available only at Dolalghat (from 2006 to 2008).

First, calibration was carried out for Melamchi subbasin (Fig. 2c, subbasin n. 3). The parameters found therein were used also for the Larke and Yangri subbasins (Fig. 2c, subbasins n. 1 and 2), with similar characteristics. After calibrating stream flow of the upstream gauge (Helambu station), calibration was run for the downstream gauge (Dolalghat station). The results obtained from the calibration at basin outlet were applied to the remaining subbasins (subbasins n. 4 to 12, Fig. 2c). The performance of the model was evaluated via mean percentage error *Bias*, Nash–Sutcliffe Efficiency (*NSE*) and squared correlation coefficient ($\rho^2$). Given the lack of site specific yearly crop yield data, the crop model was calibrated by comparison against mean yield values reported in the IWMI (International Water Management Institute) report (Bhattarai et al., 2002) for the Indrawati basin. For calibration, some most sensitive parameters related to plant morphology and phenology were tuned starting from reference values from literature.

### 2.5. Climate projections from GCMs

General circulation models (hereon, GCMs) are physically based tools that can provide meteorological variables as output. GCMs cannot represent several processes leading to precipitation occurring at a resolution smaller than the grid size, and downscaling is necessary to improve the quality of GCMs output (Groppelli et al., 2011a). Three coupled GCM models were used for this study (Fig. 3, Table 3), namely CCSM4 (Gent et al., 2011, https://www.earthsystemgrid.org), ECEarth (Hazeleger et al., 2011, http://ecearth.knmi.nl/) and ECHAM6 (Stevens et al., 2013, http://cera-www.dkrz.de). The authors have used these three models, either in the present or former versions, in a number of studies in Europe,

**Table 2**
Crop calendar used for crop yield simulation in Indrawati basin.

| Alt [masl] | Subbasin | Spring rice | Monsoon rice | Maize | Winter wheat |
|---|---|---|---|---|---|
| 600–900 | 8; 11 | 22 Mar to 07 Jul | 16 Jul to 15 Nov | 08 May to 15 Aug | 22 Nov to 07 Apr |
| 900–1200 | 9; 10; 12 | 08 Apr to 15Jul | 16 Jul to 30 Nov | 01 Apr to 21 Jul | 07 Nov to 15 May |
| 1200–1800 | 6; 7 | – | 07 Jun to 07 Dec | 16 Mar to 21 Jul | 01 Nov to 30 May |
| 1800–2200 | 4; 5 | – | 07 Jun to 07 Dec | 22 Feb to 07 Aug | 22 Oct to 15 Jun |

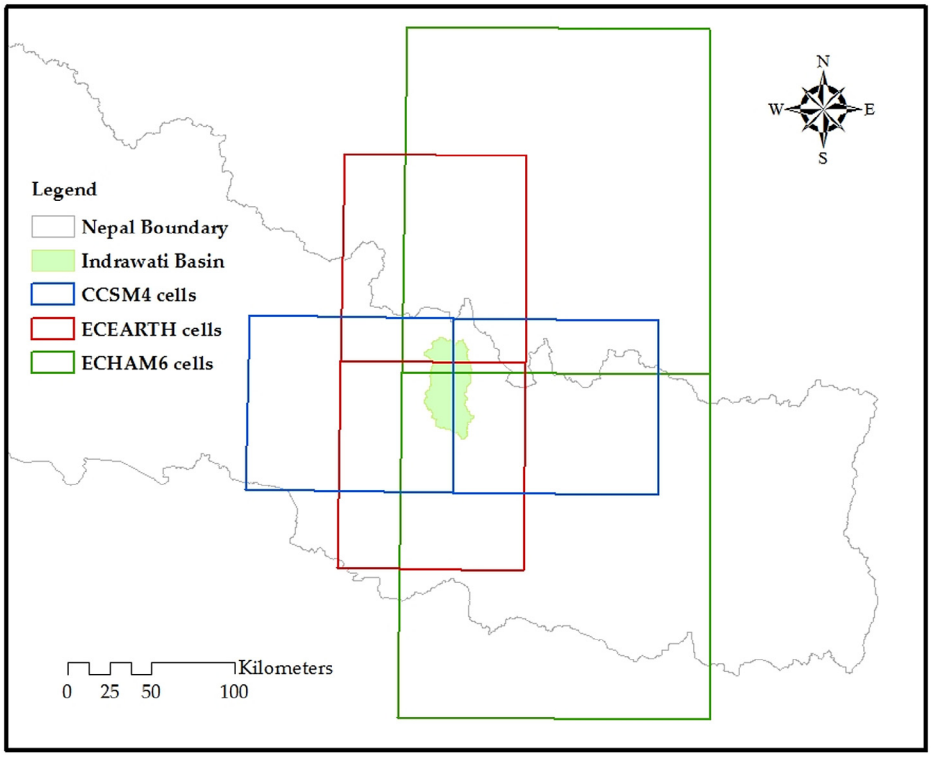


**Fig. 3.** Grid of the chosen GCMs.

**Table 3**
Main properties of the GCM models used here.

| Model | Research centre | Grid size[°] | N. cells | Layers |
|---|---|---|---|---|
| CCSM4 | Nat. Center for Atmospheric Research, USA | $1.25° \times 1.25°$ | $288 \times 144$ | 26 |
| EC-Earth | Europe-wide consortium, EU | $1.125° \times 1.125°$ | $320 \times 160$ | 62 |
| ECHAM6 | Max Planck Institute for Meteorology, GER | $1.875° \times 1.875°$ | $192 \times 96$ | 47 |

and Asia, and have set up and used specific downscaling techniques that allow to provide acceptable representation of the local climatic behavior (Bocchiola et al., 2011, 2013; Confortola et al., 2014; Groppelli et al., 2011a, 2011b; Soncini and Bocchiola, 2011). The Representative Concentration Pathways (RCPs) are greenhouse gas concentration trajectories developed in the climate modeling community, and adopted in the IPCC's Fifth Assessment Report AR5. The pathways describe projections of the components of radiative forcing, which is the change in the balance between incoming and outgoing radiation to the atmosphere, depending primarily on changes in atmospheric composition (IPCC, 2013). The scenario set containing emission, concentration and land-use trajectories is composed of four RCPs (RCP 2.6, RCP 4.5, RCP 6, and RCP 8.5) that were defined according to their range of radiative forcing values in the year 2100 (+2.6, +4.5, +6.0 and +8.5 W/m$^2$, respectively). Here, three RCPs (2.6, 4.5, 8.5) were used, with RCP4.5 and RCP6.5 being somewhat similar. Downscaling of the GCMs output of precipitation and temperature was pursued using state of the art statistical downscaling methods (Groppelli et al., 2011b). Daily precipitation from the GCMS was downscaled using Stochastic Space Random Cascade (SSRC) approach (*e.g.* Bocchiola, 2007; Bocchiola and Rosso, 2006). This method showed good performance in downscaling daily precipitation from GCM models that are normally weak in mimicking measured daily precipitation. After downscaling using SSRC, daily precipitations from GCMs possess proper average, and second order statistics (*i.e.* variance), thus being usable for unbiased development of climatic projections (for explanation of the method, see Groppelli et al., 2011a). This method involves two main steps, namely *Bias* correction, and spatial disaggregation of precipitation. Model calibration was carried out using a series of 26-year (1980–2005) observed daily precipitation data from the 12 rain gauges within the watershed. The SSRC downscaling method was calibrated for each of the available rainfall stations. Multiplicative *Bias* removal of the GCM precipitation (*i.e.* to fit with stations' average rainfall) was carried out seasonally, and subsequently the intermittence parameter of the random cascade (regulating dry spells duration), and the random noise parameter (regulating precipitation intensity) were seasonally calibrated for each station. So doing, GCMs' precipitation could be downscaled to each of the precipitation stations, and subsequently redistributed against altitude according to the lapse rate above. Downscaling of temperatures is achieved by comparison of mean seasonal temperatures gauged at the local stations against the mean values derived from GCMs. The difference ($\Delta T$) between average values is used to correct the future temperatures provided by climate models. Model calibration was carried out using a series of 26-year (1980–2005) observed daily mean temperature data from the 2 temperature gauges within the watershed. Temperatures in the catchment are then extrapolated in the SWAT model at different altitudes using the lapse rate above.

### 2.6. Hydrological and crop yield projections

Using the calibrated SWAT model, fed with the weather inputs as from the three considered GCM models (and three RCPs), we simulated potential in stream fluxes (at Dolalghat), and potential basin wide crop yield of rice, maize, wheat for the two reference decades 2045–2054 (hereon, 2050), and 2085–2094 (hereon, 2090), to be benchmarked against a control decade (1995–2004, henceforth referred to as CO). So doing, we obtained nine potential scenarios of water resources availability and crop yield. We assumed no changes of management operation and land use until 2010, while the climate input and concentration of $CO_2$ were set according to values estimated by each model and each RCP.

## 3. Results

### 3.1. Hydrological fluxes and crop yield from SWAT model

A summary of calibration and validation results of the model is reported in Table 4, and in Figs. 4 and 5.

Concerning in stream flow, the model performed relatively well at both daily and monthly scales. Acceptable *NSE* values (>0.7) demonstrated a reasonable agreement between observed and simulated flows, and noticeable values of $\rho^2$ (>0.7) indicate considerable correlation between the two. The *Bias* of simulated annual discharge from the observed discharge was low, except for the analysis of the monthly simulation (1975–1990) at basin outlet, where the model underestimated by –9% in stream flows. At monthly time step the model was more accurate, especially at basin outlet (Dolalghat, *NSE* = 0.94, $\rho^2$ = 0.95). At Melamchi basin, the peak flow was considerably underestimated during 2004, and overestimated during 2008. Sometimes peak discharges were not captured at Dolalghat. However, model calibration and validation were more accurate at basin outlet. Upper sub-catchments did not have meteorological stations, so rainfall (and snowfall) patterns are more uncertain, which might have made the results worst. In Fig. 5 the results obtained from calibration of crop yield are shown, and in Table 5 calibration parameters are reported, displaying slight variations from the default values from literature. The mean value of crops yield coming from IWMI (International Water Management Institute) report (Bhattarai et al., 2002) were first compared to the mean production for Nepal in year 2010–2011 (Aryal et al., 2011). The national crop production in 2010–2011 showed an average yield of 2.98 ton ha$^{-1}$ of rice, 2.28 ton ha$^{-1}$ of maize, and 1.12 ton ha$^{-1}$ of wheat. These are in agreement with IWMI Report (namely, 2.75 ton ha-1, 2.45 ton ha$^{-1}$ and 1.70 ton ha$^{-1}$, respectively). The mean crop yields during 1995–2004 as simulated by SWAT appear in reasonable agreement with these reported statistics, with possibly some underestimation for wheat (2.45 ton ha$^{-1}$, 2.52 ton ha$^{-1}$ and 1.17 ton ha$^{-1}$, respectively).

**Table 4**
Indrawati basin. SWAT hydrological calibration and validation results.

| Station | Variable | NSE [.] | | $\rho^2$ [.] | | Mean annual flow [m$^3$ s$^{-1}$] | | |
|---|---|---|---|---|---|---|---|---|
| | Period | Daily | Monthly | Daily | Monthly | Obs. | Sim. | Bias [%] |
| Helambu | 2001–2008 (calib) | 0.72 | 0.77 | 0.72 | 0.77 | 10.6 | 10.4 | –1.43 |
| Dolalghat | 1975–1990 (calib) | – | 0.85 | – | 0.87 | 91.4 | 83.1 | –9.14 |
| | 2006–2008 (valid) | 0.87 | 0.94 | 0.87 | 0.95 | 80.6 | 79.4 | –1.46 |

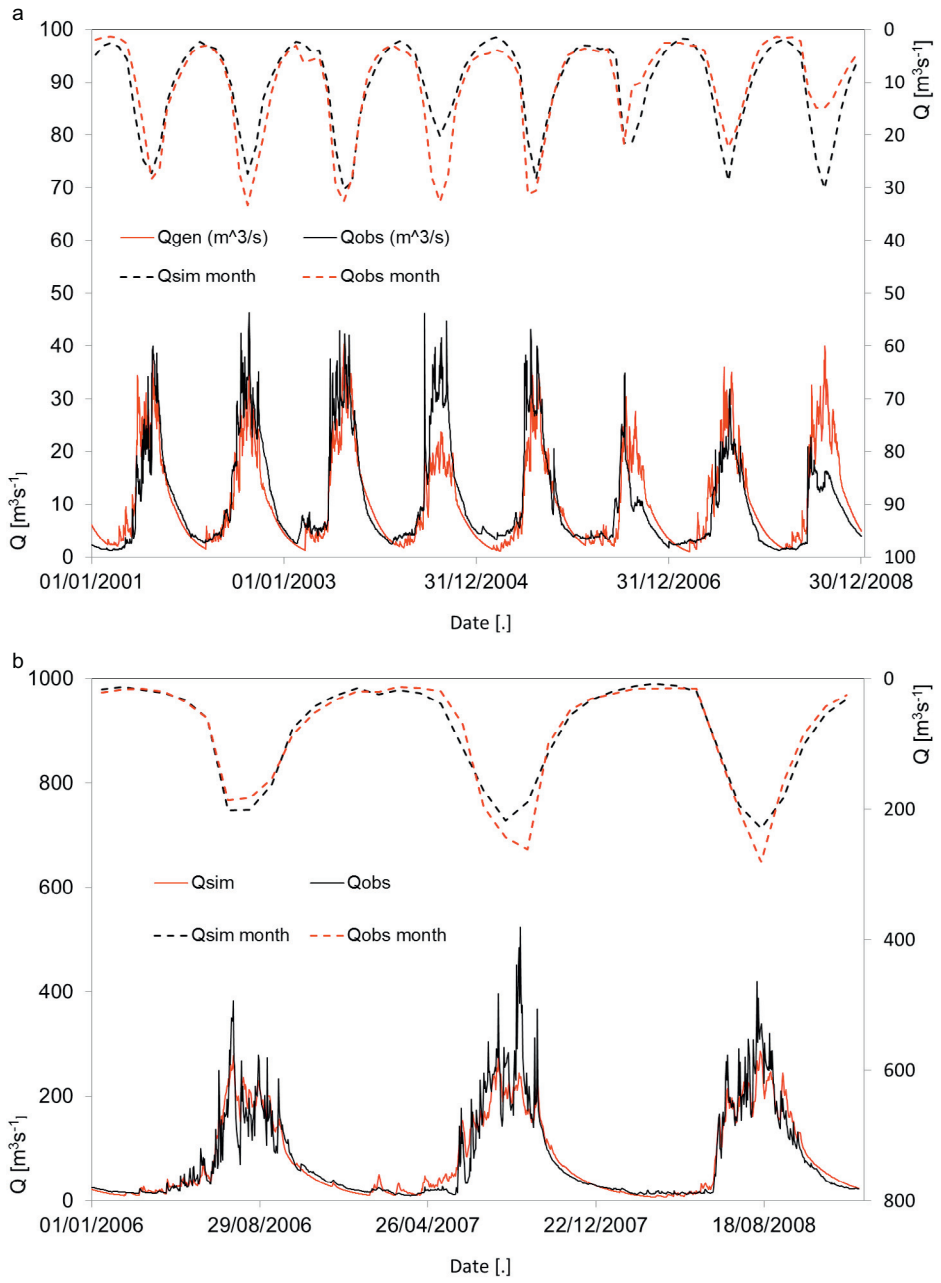


**Fig. 4.** SWAT hydrological calibration and validation. (a) Daily hydrograph at Melamchi outlet, period 2001–2008 (calibration). (b) Daily hydrograph at Indrawati outlet, period 2006–2008 (validation).

### 3.2. *Future climate scenarios*

In Table 6, the main results of future climate scenarios projection are presented. Therein, we report the $CO_2$ atmospheric concentration adopted within the GCM models, and provided from the RCP Database (Version 2.0.5) website. As suggested by the SWAT model manual (Arnold et al., 2010), $CO_2$ during the control period was taken as a default value of ambient concentration of 330 ppm. Since SWAT allows us to enter a maximum value of 800 ppm of $CO_2$, this value was adopted to simulate decade 2085–2094 related to RCP 8.5, instead of 844.80 ppm, projected in RCP Database. In Table 6 we report the values of seasonal temperature, precipitation, and $CO_2$ (the latter constant) on the catchment, as projected by the three models under the three RCPs used here, after downscaling, against the CO period as measured in reference ground stations.

Temperature increase is expected in all scenarios, and the greatest increase is expected under RCP 8.5. Some decreasing trends are projected by CCSM4. Winter temperature under RCP 2.6 displays a decrease in 2050, and 2090, and also a slight reduction in 2050 under RCP 4.5. Under RCP 4.5 and 8.5, the highest rise in temperature would emerge during Winter and Spring, except for CCSM4, where warming would be more pronounced in Spring and Summer. ECHAM6 projected a largest increase in Winter, while in any other season temperature was expected to rise the most by CCSM4, under all RCPs.

### 3.3. *Future flow scenarios*

Future projected monthly flows as simulated by SWAT, with relative error bars (5%), are reported in Fig. 6. Generally mean monthly

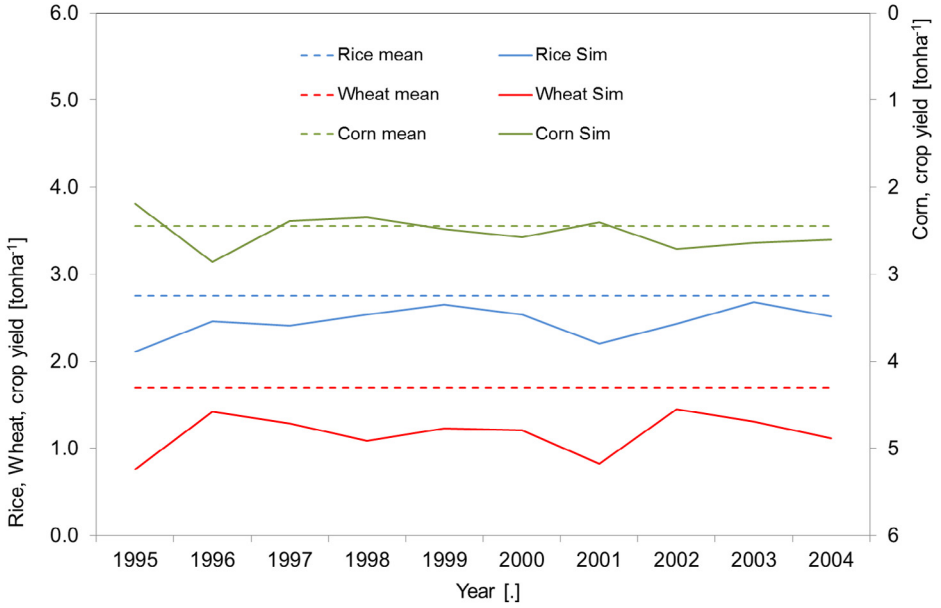


**Fig. 5.** Simulated yield of rice, wheat, and maize against mean yield from IWMI report (Bhattarai et al., 2002, see section 2.4).

discharge presented a variation of nearly 20% from the CO period values. The largest variation was given by CCSM4 (Fig. 6a) climate input, with largest increase in Autumn and Winter (September to February) during 2045–2054, under RCP 2.6. The outputs of ECHAM6 (Fig. 6c) reduced annual river discharge in every decade and RCP, except under RCP 4.5 in 2050, while a more variable pattern (either decreasing or decreasing discharge also for different months) was seen using ECEarth (Fig. 6b).

### 3.4. Future crop yield scenarios

Prospectively modified temperature, precipitation, and $CO_2$ concentration under climate change scenarios drove some changes in annual yield of our three crops in Indrawati basin. Average values for each decade, GCM model, and RCP are reported in Fig. 7. Rice (Fig. 7a) clearly tends to remain slightly higher than during the CO period in both the reference decades, for all GCMs, and RCPs. Sole exception is the ECHAM6 model at 2090, under all RCPs. Projected maize yield is more variable. CCSM4 always projected decreasing maize yield, especially in 2050, under all RCPs. ECEarth model projected substantially constant (slightly either decreasing or increasing), while ECHAM6 depicted maize yield as increasing at 2050, but decreasing at 2090, under all RCPs. Concerning wheat, CCSM4 projected decreased yield, differently for each RCP, and decade, with 2050 having a minimum, and 2090 displaying slight increase. ECEarth always depicted yield as increasing, while ECHAM6 depicted constant yield at 2050, and decreasing yield at 2090.

## 4. Discussion

### 4.1. SWAT model performance

The SWAT model could be set up and tuned to mimic reasonably well stream flows of the Indrawati basin. From Fig. 4a, some criticalities arise in depicting flows at Helambu station for some years (*e.g.* in 2008). Clearly from Fig. 2b and c, precipitation in the Helambu basin (subbasin 3) is not measured, but rather extrapolated from stations at lower elevations, possibly leading to inaccurate depiction of hydrological cycle. Fig. 4b shows a somewhat better agreement of SWAT modeled discharges against observations at Dolalghat (*e.g.* for year 2008), unless for some peaking discharge values during Summer. The lack of distributed information of temperatures may have impacted the hydrological simulation, because temperature regulates snow fall, and snow melt at thaw, and evapotranspiration.

The simulated crop yields from the SWAT model are benchmarked against available literature data, providing approximate average values. Fig. 5 displays that maize, and possibly rice are well depicted, while wheat is somewhat underestimated. In spite of the slight disagreement here, we may assume that the SWAT model can be used here to assess the potential impact of future weather patterns as from GCMs on crop yield.

**Table 5**
Indrawati basin. SWAT crop yield calibration parameters.

| Parameter | Definition | Rice | | Corn | | Wheat | |
|---|---|---|---|---|---|---|---|
| | | Default | Calib. | Default | Calib. | Default | Calib. |
| *HVSTI* | Harvest index [kgha$^{-1}$/(kgha$^{-1}$)] | 0.5 | 0.6 | 0.5 | 0.43 | 0.4 | 0.5 |
| *WSYF* | Lower limit of harvest index [kgha$^{-1}$/(kgha$^{-1}$)] | 0.25 | 0.5 | 0.3 | 0.25 | 0.2 | 0.45 |
| *BLAI* | Maximum potential leaf area index [m$^2$ m$^{-2}$] | 5 | 5 | 6 | 5 | 4 | 4 |
| *BIO_E* | Radiation use efficiency [kgha$^{-1}$ MJ$^{-1}$ m$^2$] | 22 | 22 | 39 | 35 | 30 | 30 |
| $T_{base}$ | Minimum temperature for growth [°C] | 10 | 10 | 8 | 10 | 0 | 0 |
| $T_{opt}$ | Optimal temperature for growth [°C] | 25 | 25 | 25 | 25 | 18 | 18 |

**Table 6**
Indrawati basin. Projected $CO_2$ concentration per decade according to the chosen RCPs. Projected average seasonal temperatures *vs* CO in reference station 1043, and seasonal average cumulated precipitation *vs* CO in reference station 1018.

| RCP (decade) | | 2.6 (2050) | | | 4.5 (2050) | | | 8.5 (2050) | | |
|---|---|---|---|---|---|---|---|---|---|---|
| $CO_2$ | 330 | 443 | | | 487 | | | 540 | | |
| T | CO | CCSM4 | ECEarth | ECHAM6 | CCSM4 | ECEarth | ECHAM6 | CCSM4 | ECEarth | ECHAM6 |
| JFM | 10.4 | 9.2 | 10.9 | 11.7 | 10.2 | 11.4 | 11.6 | 10.8 | 11.9 | 13.0 |
| AMJ | 18.0 | 16.6 | 19.0 | 18.8 | 17.8 | 19.8 | 20.1 | 18.1 | 20.2 | 20.4 |
| JAS | 18.8 | 20.2 | 19.8 | 19.4 | 20.6 | 20.5 | 20.3 | 20.7 | 20.5 | 21.2 |
| OND | 12.9 | 16.5 | 13.9 | 13.5 | 16.9 | 14.1 | 14.0 | 17.5 | 14.9 | 14.7 |
| Year | 15.0 | 15.6 | 15.9 | 15.9 | 16.4 | 16.5 | 16.5 | 16.8 | 16.9 | 17.3 |
| | | 2.6 (2090) | | | 4.5 (2090) | | | 8.5 (2090) | | |
| T | CO | CCSM4 | ECEarth | ECHAM6 | CCSM4 | ECEarth | ECHAM6 | CCSM4 | ECEarth | ECHAM6 |
| $CO_2$ | 330 | 426 | | | 534 | | | 845(800) | | |
| JFM | 10.4 | 9.7 | 10.5 | 10.7 | 11.2 | 12.0 | 12.9 | 13.5 | 14.5 | 16.0 |
| AMJ | 18.0 | 17.7 | 18.7 | 17.9 | 18.8 | 20.7 | 20.7 | 21.3 | 22.6 | 23.9 |
| JAS | 18.8 | 19.9 | 19.7 | 20.1 | 20.7 | 20.7 | 21.2 | 22.5 | 22.6 | 23.6 |
| OND | 12.9 | 15.0 | 13.4 | 13.0 | 16.1 | 15.0 | 14.5 | 18.3 | 17.1 | 16.8 |
| Year | 15.0 | 15.7 | 16.3 | 16.2 | 16.9 | 17.8 | 18.3 | 19.1 | 19.9 | 21.2 |
| RCP (decade) | | 2.6 (2050) | | | 4.5 (2050) | | | 8.5 (2050) | | |
| P | CO | CCSM4 | ECEarth | ECHAM6 | CCSM4 | ECEarth | ECHAM6 | CCSM4 | ECEarth | ECHAM6 |
| JFM | 104.2 | 331.2 | 108.9 | 74.7 | 169.0 | 84.6 | 162.4 | 89.0 | 35.8 | 58.0 |
| AMJ | 179.8 | 111.4 | 190.7 | 151.3 | 98.0 | 190.6 | 113.1 | 104.8 | 191.3 | 117.9 |
| JAS | 188.2 | 234.3 | 171.4 | 173.3 | 275.2 | 196.6 | 195.2 | 292.2 | 181.2 | 176.5 |
| OND | 128.8 | 614.3 | 87.3 | 88.4 | 560.0 | 23.8 | 175.0 | 485.2 | 147.8 | 86.1 |
| Year | 1803 | 3873 | 1675 | 1463 | 3306 | 1487 | 1937 | 2914 | 1668 | 1315 |
| RCP (decade) | | 2.6 (2090) | | | 4.5 (2090) | | | 8.5 (2090) | | |
| P | CO | CCSM4 | ECEarth | ECHAM6 | CCSM4 | ECEarth | ECHAM6 | CCSM4 | ECEarth | ECHAM6 |
| JFM | 104.2 | 206.9 | 78.0 | 127.4 | 274.0 | 89.3 | 65.6 | 235.9 | 58.9 | 86.9 |
| AMJ | 179.8 | 144.3 | 202.7 | 107.6 | 144.9 | 200.5 | 119.5 | 117.7 | 230.3 | 81.4 |
| JAS | 188.2 | 243.6 | 175.7 | 179.1 | 253.5 | 183.2 | 203.6 | 264.7 | 187.0 | 188.8 |
| OND | 128.8 | 200.2 | 109.6 | 94.9 | 168.2 | 132.6 | 103.3 | 315.8 | 117.3 | 193.5 |
| Year | 1803 | 2385 | 1698 | 1527 | 2521 | 1817 | 1476 | 2802 | 1781 | 1652 |

### *4.2. Climatic and hydrological scenarios*

Substantially all GCMs depict a warming weather until half century, and further at the end of century. The only exception is given by the CCSM4 model, projecting a decrease in temperature in Winter and Spring at 2050 and 2090 along RCP 2.6, and (very slight) decreasing temperature in Winter and Spring at 2050 along RCP 4.5, but increasing rapidly ever after. Precipitation patterns are indeed more variable. The CCSM4 model depicts a very large (possibly unreasonable) increase of precipitation at 2050 (3873 mm $y^{-1}$, RCP 2.6 to 2914 mm $y^{-1}$, RCP 8.5 *vs* 1803 mm $y^{-1}$ in CO period), mostly given by a large increase (three times as much as the CO period) during Winter and Fall. However, precipitation tends to decrease quickly in CCSM4 projections until 2090, albeit always larger than the CO run. Both ECEarth and ECHAM6 depict a substantially decreasing pattern of precipitation until 2050 and 2090, with difference as per the different RCPs and the season.

Few studies were carried out hitherto, focusing upon future climate of Nepal, which can be used as a benchmark here. Agrawala et al. (2003) examined the results of the OCDE Development and Climate Change project for "Development and climate change in Nepal: focus on water resources and hydropower", where climate change scenarios (until 2100) for the entire Nepal were assessed, using MAGICC/SCENGEN suite of 7 best performing (out of 17) GCM models under the B2 SRES scenario (Houghton et al., 2001). They found a projected change of average yearly temperature (against 1977–1994) in the order of +1.7 °C until 2050, and of +3.0 °C until 2100 (here, on average under the RCP4.5, qualitatively comparable to B2 scenario moderately optimistic, we found +1.4 °C until 2050, and +2.6 °C until 2090). Precipitation changes in Agrawala et al. (2003) were cast as +7.3% until 2050 and +12.6% until 2090 (yearly precipitation in baseline period 1433 mm $y^{-1}$), with large deviations from one another. Here we found on average under RCP4.5 +24.4% until 2050 and +7.5% until 2090, although with a large spread. Karmacharya et al. (2007) used REGCM3 model (Giorgi, 1990) to project Nepal climate under A2 SRES scenario until 2070 (average 2039–2069). Considering East Nepal here, they projected an increase (*vs* 1961–1990) of temperature of +1.9 °C yearly (here, +2 °C by 2050 under RCP8.5, comparable to A2, scenario pessimistic or *business as usual*), +2.1 in Winter (here, +1.5 °C), and +1.9 °C in monsoon season (here, +2 °C in Summer). Precipitation in Agrawala et al. (2003) was projected to decrease by –9.6% in Winter, –18.1%in monsoon season, and –13.2% annually. Here, we found on average –41.6% in Winter, +15% in Summer, and +9.5% yearly, but with CCSM4 providing large increase in Summer and Fall (thence, yearly). Considering only ECEarth and ECHAM6, one has –54% in Winter, –5% in Summer, and –17.3% yearly, somewhat more consistent with the results above. A largest spread is seen for CCSM4 model for precipitation during Winter and Fall until 2050. Accordingly, more uncertainty may be expected therein.

In projecting hydrological cycle and crop yield until 2100 we had to rely on the assumption that the model calibrated against past records is applicable to future conditions, which is a critical assumption. This limitation needs to be kept in mind when commenting our results. Fig. 6 reports modified monthly stream flows at Dolalghat closure section, benchmarked against CO period (1995–2004). CCSM4 model (Fig. 6a) predicts large increase of stream flows until 2050, and slightly decreasing until 2090, and somewhat larger for RCP8.5. This results from the considerable increase of precipitation by CCSM4 during Fall until 2050, and to a smaller degree in Summer (Table 6), with September displaying large precipitation increase. Larger precipitation at Fall and Winter implies larger

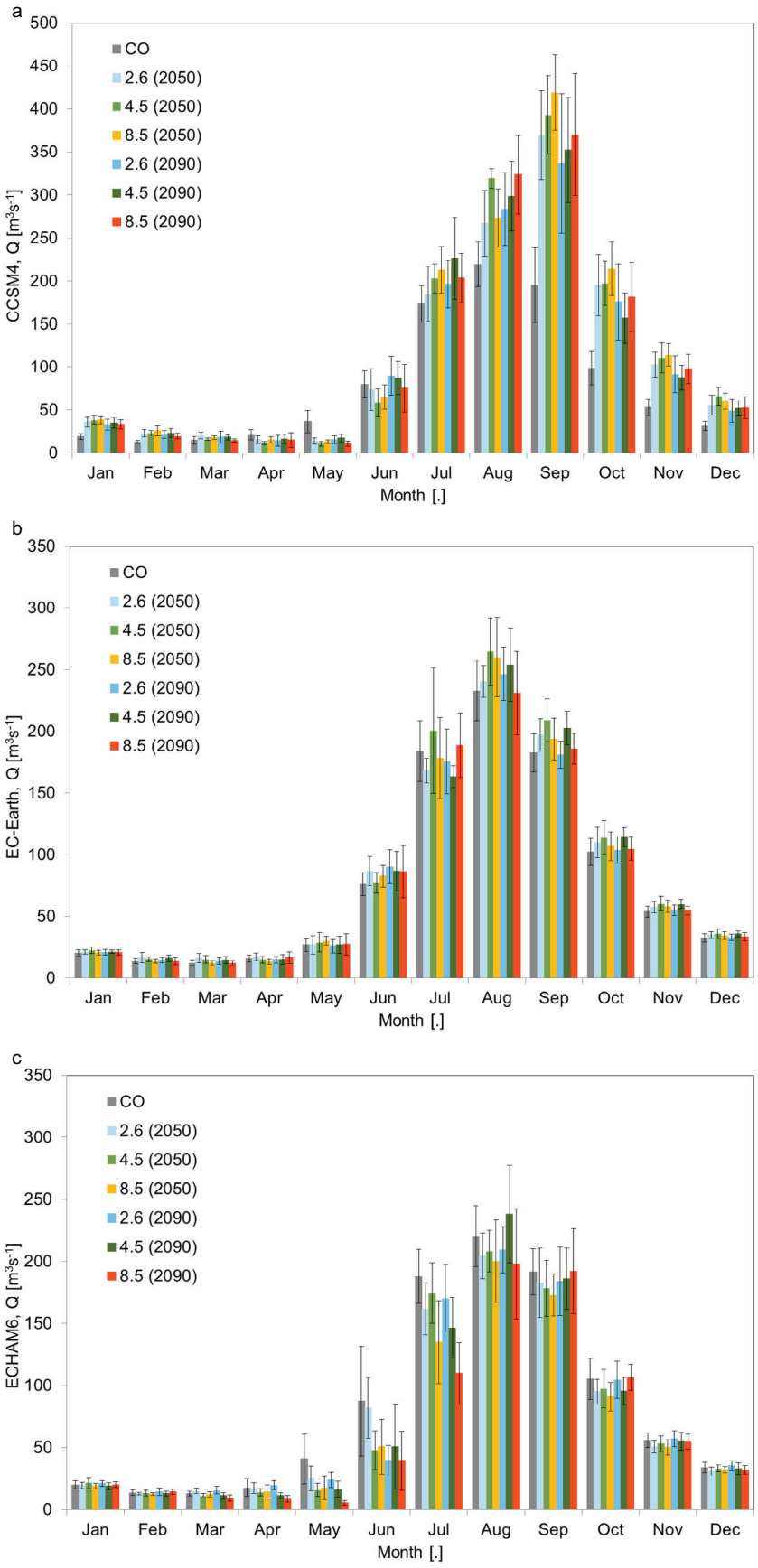


**Fig. 6.** Indrawati basin closed at Dolalghat. Future projected monthly average stream flow per decade and RCP *vs* CO period. (a) CCSM4. (b) ECEarth. (c) ECHAM6. Notice a different scale on the *y* axis for CCSM4.

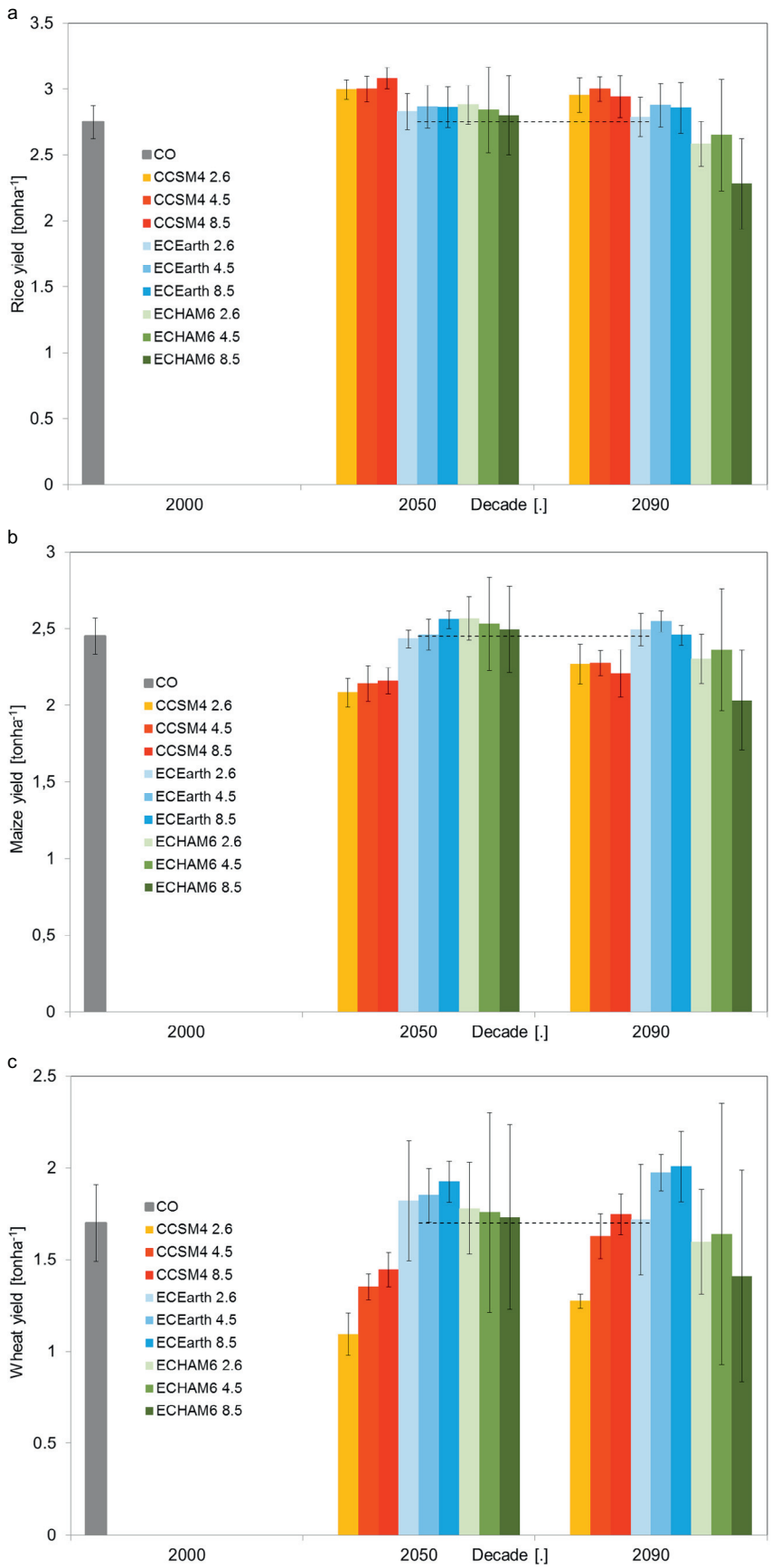


**Fig. 7.** Future projected average crop yield per decade, GCM and RCP *vs* CO period. (a) Rice. (b) Maize. (c) Wheat. Notice a different scale on the *y* axis for each crop.

accumulation of snow at the highest altitudes (subbasins 1–3, Fig. 2c), which in turn sustains in stream flows at thaw, occurring at the highest altitude until September. The yearly average projected runoff at 2050 is of 113.9 $m^3 s^{-1}$ under RCP2.6 (RCP4.5, 120.6 $m^3 s^{-1}$, RCP8.5, 122.3 $m^3 s^{-1}$), and at 2090 it is 110.4 $m^3 s^{-1}$ under RCP2.6 (RCP4.5, 114.3 $m^3 s^{-1}$, RCP8.5, 116.4 $m^3 s^{-1}$), against 81. 9 $m^3 s^{-1}$ of CO run. Error bars are considerably larger for some of the projected scenarios, thus implying less predictability and larger potential for high flows (and floods).

ECEarth (Fig. 6b) depicts substantially unchanged discharge, with monthly difference as per different RCPs, with no clear pattern. However one can notice larger error bars than in the CO run, in this case leading to potential for lower floods and possibly droughts. The yearly average projected runoff at 2050 is of 82.7 $m^3 s^{-1}$ under RCP2.6 (RCP4.5, 88.1 $m^3 s^{-1}$, RCP8.5, 83.7 $m^3 s^{-1}$), and at 2090 it is 81.3 $m^3 s^{-1}$ under RCP2.6 (RCP4.5, 84.2 $m^3 s^{-1}$, RCP8.5, 81.3 $m^3 s^{-1}$), substantial-ly unchanged against CO. This seems expected, given the substantially unchanged (albeit slightly decreasing) precipitation patterns under all RCPs for ECEarth.

Under ECHAM6, Winter CO values are substantially met, while in Spring and monsoon season (especially in June and July) in stream discharge is largely decreasing. This stems from the low precipitation by ECHAM6 during Spring and early Summer (Table 6). Here, the yearly average projected runoff at 2050 is of 74.8 $m^3 s^{-1}$ under RCP2.6 (RCP4.5, 72.5 $m^3 s^{-1}$, RCP8.5, 67.4 $m^3 s^{-1}$), and at 2090 it is 74.6 $m^3 s^{-1}$ under RCP2.6 (RCP4.5, 73.0 $m^3 s^{-1}$, RCP8.5, 65.8 $m^3 s^{-1}$), visibly lower (until –20%) than CO run. Again here, larger variation is expected than in Summer. The variability of the hydrological projections stems from the variability of the precipitation scenarios. This is witnessed also in the present literature concerning future hydrological cycle and cropping systems worldwide (*e.g.* Bavay et al., 2009; Bocchiola et al., 2011, 2013; Confortola *et al.*, 2014; Groppelli et al., 2011b; Immerzeel et al., 2010; Olesen et al., 2007). Here, precipitation is the strongest driver of the hydrological cycle, because little buffer is provided by the snow and glacier cover, as often seen in the southern Himalayas (Kaser et al., 2010; Konz et al., 2007), and precipitation feeding is much larger with respect to the northern Himalayas (*e.g.* in the much drier Karakoram, Bocchiola et al., 2011; Winiger et al., 2005). Scientific effort should be there-fore focused on developing methods for reducing the uncertainty of future precipitation assessment.

### *4.3. Rice yield scenarios*

Fig. 7a reports potential future rice yield. Within Indrawati basin both Spring paddy and Summer paddy (also called monsoon paddy, Table 2) are cultivated, which were lumped here. Summer rice was cultivated in all subbasins, whereas Spring rice was grown only below 1200 masl. Rice is a C3 plant, so an increase in $CO_2$ (Table 6) may increase yield. ECHAM6 predicts a noticeable decrease until 2090, and more so for increasing RCP (down to –17%). This stems from decrease in precipitation during Spring and Summer, especially under RCP8.5. The largest decrease at 2090 under RCP8.5 was induced by a temperature increase of +4.8 °C and a mean value of 11.41 water stress days during the rice growth season. Rice yield in Fig. 7a is averaged on the whole catchment, and yet some variability was seen depending on altitude. For instance, in subbasin 9 (Fig. 2c), rice production increased by +19.35% until 2090 under RCP4, and by +20.67% and +40.49% (about 1 ton $ha^{-1}$), until 2050 and 2090 under RCP8.5 (not shown for shortness). Biomass stopped growing one month earlier than in CO due to the increase in temperature, but with larger yield. Other subbasins higher than subbasin 9, *i.e.* subbasin 4, 6 and 7 had shorter growth periods, and yield was reduced according to the general trend. Variability at subbasin scale may be impacted by poor depiction of climate patterns (especially temperature), and yet it is worth noticing large potential changes in cropping systems due to large topographic gradients in this area.

SWAT model accounts for the effect of $CO_2$ upon biomass production using the method by Stöckle et al. (1992), valid approximately within the range 330–660 ppm. It is not actually known what may happen for higher concentration of $CO_2$, such as projected under RCP8.5 (*i.e.* 845, set to 800). Recent studies based upon controlled experiments (free air $CO_2$ experiments FACE, *e.g.* Kim et al., 2003; McMurtrie et al., 2008) demonstrated that for $CO_2$ concentration, as high as 700 ppm biomass growth of plants (including rice) may be modified (*i.e.* either amplified or reduced) under water and nutrient limitation. The results provided here for RCP8.5, displaying a very large $CO_2$ concentration, may be critical in this sense. ECHAM6 displayed larger error bars than CO, indicating less dependable yield, and potentially more risk for *food security* (Torriani et al., 2007).

CCSM4 increased rice yield up to +12% under RCP8.5 in 2050, although constantly higher until 2090. This is consistent with increasing precipitation and temperature in CCSM4 under all RCPs. On the other hand, under RCP 8.5, precipitation was almost unchanged between 2050 and 2090, and relative decrease of rice yield was driven by increase of temperature. Rice growth season became warmer until 2090, with +4.6 °C *vs* CO in Spring, hampering rice growth, and then decreasing production (from +12.1% to +7.0%). Subbasin 4 (Fig. 2c), the highest with cropping (1800–2200 masl), had decreasing rice yield in all projections with CCSM4 (not shown). Biomass growth therein stopped sooner than in CO, by one month (*i.e.* September) in 2050 and 2090 for all RCPs, and by two months (*i.e.* August) in 2090 for RCP 8.5. This was due to warmer conditions in this high altitude area during 2050 (+2.5 to +3 °C *vs* CO) and 2090 (+2.6 to +4.5 °C *vs* CO) for all RCPs. ECEarth model projected slight increase of rice yield. The same behavior of subbasin 4 reported above for CCSM4 was seen in ECEarth, with a decrease of –27.4% in 2090 for RCP 8.5.

Rice production seems somewhat robust in the face of poten-tial climate change in the next century. If one takes as more likely the intermediate RCP4.5, rice yield should not be largely impact-ed, besides increase year to year variability. In this sense, rice is a most suitable crop for Indrawati basin in the future. Some de-crease is expected under RCP8.5 of the ECHAM6 model, *i.e.* for large decrease of precipitation, and large increase of temperatures (making growth season shorter, according to heat units approach), only at the end of century. Also, one has to verify the potential response of rice to very high $CO_2$ concentration under RCP8.5 scenario. Po-tential adaptation strategies for future climate change may thus include larger use of irrigation to make up for water stress (*e.g.* Bocchiola et al., 2013), anticipation of sowing date, and possibly use of modified (*i.e.* slower maturing) cultivars (*i.e.* with higher heat units, *e.g.* Torriani et al., 2007; Tubiello et al., 2000), also varying with altitude. Also, potential lack of nutrients need to be verified, which we did not consider here for lack of information, together with potential land use changes in the future.

### *4.4. Maize yield scenarios*

Maize is cultivated from April/May to July/August. Maize is a C4 plant, and its productivity is less influenced by increase in $CO_2$ atmospheric concentrations (*e.g.* Bocchiola et al., 2013). Maize yield from CCSM4 (Fig. 7b) always decreased. Under RCP2.6 yield in 2050 was smaller than in 2090, and similarly under RCP4.5, in agreement with larger water stress during Spring at 2050 (Table 4). For CCSM4 Summer temperature in 2090 was in practice the same as in 2050, and even lower by –0.5 °C for RCP 2.6 (Table 6). Under RCP8.5 maize yield in 2090 was slightly lower than in 2050, because, unlike under the other RCPs, water stress was larger by the end of the century, following a large reduction of precipitation during Spring (Table 6). Subbasin 10 (Fig. 2c) showed an increasing yield in all sce-

narios (not shown), especially under RCP4.5 and RCP8.5, and by the end of the century maize yield grew by +16.2% and +30.2% respectively. This increase was coherent with temperature increase in the subbasin, by +1.7 °C in 2090 for RCP 4.5 and 8.5.

Under ECEarth model the largest increase under RCP2.6 and RCP4.5 was observed in 2090, due to slightly increased Spring precipitation. Subbasin 4 had a reduction in maize yield, larger at 2090. Temperature stress (18 temperature stress days) exceeded the mean value for the basin, and was experienced during the century under RCP4.5 and RCP8.5 at 2050 and 2090. Under ECHAM6 the largest increase was reached in 2050 under RCP2.6, while the largest decrease was at 2090 for RCP8.5. Also with ECHAM6 subbasin 4 had decreased maize yield at 2050 under RCP4.5 and RCP8.5 reduced maize productivity by –21.8% and –29.7%, respectively. This was due to an average of 19.6 temperature stress days at 2050 (RCP4.5), and of 15.8 water stress days for RCP8.5. ECHAM6 displayed here the largest error bars for all RCPs and both decades, witnessing a potential for large variability and increased risk for maize cropping.

Maize seems a most critical crop for Indrawati basin in the future. Already at half century, large decrease and increased year to year variability are expected, as a result of increasing temperatures and decreased precipitation. Toward the end of century the projected situation seems critical, with most scenarios projecting large decrease. These results are consistent with those from studies on maize worldwide (*e.g.* Bocchiola et al., 2013; Torriani et al., 2007), indicating that this highly water consuming crop may suffer largely from climate change effects. Adaptation strategies for maize cropping in the Indrawati basin will likely be necessary soon enough, including use of irrigation, change of sowing date, and possibly of different, slower maturing cultivars. Increased use of irrigation may provide increased specific (*i.e.* per kg of yield) *water footprint* for maize (*e.g.* Bocchiola et al., 2013; Nana *et al.*, 2014), potentially raising the question as to whether maize production may be feasible and sustainable in the Indrawati catchment. The approach we developed here may be used in the future to test adaptation strategies and potential sustainability of maize cropping.

### 4.5. Wheat yield scenarios

Wheat was the only Winter crop considered here, growing approximately from November to May. Much like rice, wheat is a C3 crop, positively affected by increase of $CO_2$. Under CCSM4, the largest decrease (–35.9%) occurred under RCP2.6, due to a considerable decrease in Spring temperature (Table 6). Under ECEarth model, RCP4.5 delivered an increase of +8.8% at 2050 and 16.2% at 2090, following temperatures increasing in Winter and Spring. Scenario 8.5 depicted +13.2% wheat yield at 2050 and +18.1% at 2090, due to $CO_2$ increase, higher temperatures, and increasing Spring precipitation (Table 6). Under ECHAM6, RCP 2.6 showed a slight increase of wheat yield at 2050 given by slightly warmer climate, with still acceptable precipitation, but mostly decrease thereafter.

Wheat seems the most critical crop among our three target species. At half century under all scenarios a large variability of yearly yield is seen, and sensible decrease in mean precipitation during already dry Winter and Spring may largely affect mean yield (see Bhatt et al., 2013). At the end of the century, most scenarios depict considerable decrease of precipitation and yield. Therefore, in the future, more stable production of wheat may be given by water supply from irrigation, otherwise making wheat production largely insecure. The necessary amount of water and feasibility of wheat production under future climate will require specific investigation henceforth. Again here, one has to verify the potential response of wheat to very high $CO_2$ concentration under RCP8.5 scenario.

## 5. Conclusions

Our "what if" study provided new insights into the potential fallout of global warming upon *food security* of population living in the Indrawati catchment. Notwithstanding the relative lack of weather data, especially at the highest altitudes, we could mimic the hydrological cycle of the area acceptably well. Even more sparse is the knowledge of crop productivity in the area and of its variability with topography and climate, so the SWAT model was used to provide a representative depiction of distributed crop yield within the catchment. The outputs from our chosen GCMs and RCPs consistently depict an increase of $CO_2$, and in temperature, but more variable output of precipitation. Prospective impact on crop yield is consequently variable.

Rice yield would be constant on average at the end of the century (+1%), but with a large spread between –17% (ECHAM6, RCP8.5) and +9% (CCSM, RCP4.5), and with a larger year to year variability than present. These issues are critical, and yet rice seems a suitable crop in Indrawati basin under future climate, pending enacting of adaptation strategies, most notably irrigation.

Maize yield would decrease on average by –5% at the end of the century, ranging from –17% (ECHAM6, RCP 8.5) to +4% (CCSM4, RCP4.5), again with large year to year variation. Large water requirements of maize will make it necessary to develop irrigation systems for sustainable cropping under future climate.

On average, wheat yield would decrease by –2% at 2090, but it may reach down to –25% according to CCSM4 (RCP2.6), and up to +18% according to ECEarth (RCP8.5), and under most scenarios (5 out of 9) wheat yield decreases. Wheat displays the largest year to year variability among our three crops, being the most insecure crop in this sense, and widespread irrigation systems will be utmost necessary for adaptation under climate change.

Rainfall variability between models and RCPs plays a large role in modifying crop patterns. Concerning the different RCPs, RCP2.6 and RCP8.5 depict in practice more extreme pathways (*i.e.* either very optimistic or very pessimistic). Thus, RCP4.5, which depicts an intermediate situation, may be taken as more credible. The modeling tool we built here provides a way to investigate potential adaptation strategies under future climate scenarios, including use of water for irrigation, cultural practices (*e.g.* sowing and harvesting dates), land use changes, and use of different cultivars. Also, nutrient dynamics and manuring will need be explored, given that nutrient lacking may hamper present crop production. The response of crops to climate change may vary with altitude, so in the future crop dynamics will be investigated in this respect, and adaptation strategies explored accordingly. Our results show that climate change may put at stake *food security* in the Indrawati catchment and in the high altitude areas of Nepal in the near and mid-term future. Food demand in the country is going to increase due to the growing population and consumption patterns, and increasing crop yield is needed. Our work here may contribute to assessment of future food security in this delicate area, and to initiate planning of adaptation under a scientifically driven, quantitative framework, that, uncertain as it may be, can indeed provide guidance to policy makers.

## Acknowledgments

Dr. Eng. Andrea Soncini, and Eng. Gabriele Confortola, at Politecnico di Milano, are kindly acknowledged for helping with GCMs data treatment. Eng. Ester Nana acknowledges support from the Share-Stelvio project funded by Lombardia Region, and Dr. Daniele Bocchiola acknowledges support from the I-CARE project funded by Politecnico di Milano, and from the Khumbu hydrology project funded by EVK2-CNR committee of Italy. The paper reports work of the leading author, Eng. Irene Palazzoli at UNESCO-IHE, under

the umbrella of the project Adaptation to Global Change in Agricultural Practices (AGloCAP) supported by the Dutch Development Cooperation. Two anonymous reviewers are gratefully acknowl-edged for their positive comments and for helping in improving the paper.

## References


Agarwal, A., Babel, M.S., Maskey, S., 2014. Analysis of future precipitation in the Koshi River basin, Nepal. J. Hydrol. http://dx.doi.org/10.1016/j.jhydrol.2014.03.047.

Agrawala, S., Raksakulthai, V., van Aalst, M., Larsen, P., Smith, J., Reynolds, J., 2003. Development and Climate Change in Nepal: Focus on Water Resources and Hydropower, COM/ENV/EPOC/DCD/DAC(2003)1/FINAL. OECD Press, France.

Arnold, J., Kiniry, J., Srinivasan, J.W., Haney, E., Neitsch, S., 2010. Soil and water assessment tool input/output file documentation (version 2009). Grassland, Soil and Water Laboratory-Agricultural Research Service; Blackland Reasearch Centre-Texas Agrilife Research.

Arnold, J.G., Moriasi, D.N., Gassman, P.W., Abbaspour, K.C., White, M.J., Srinivasan, R., et al., 2012. SWAT: model use, calibration, and validation. Trans. ASABE 55 (4), 1491–1508.

Aryal, B.P., Regmi, H., Sah, S.N., Acharya, K., Rimal, U.H., Pahari, K., et al., 2011. *Crop Situation Update (A joint assessment of 2010 summer crops and outlook for 2011 winter crops)*, s.l.: Ministry Of Agriculture And Cooperatives, World Food Programme, Food And Agriculture. Organization. <http://documents.wfp.org/stellent/groups/public/documents/ena/wfp234049.pdf>.

Awasthi, K.D., Sitaula, B.K., Singh, B.R., Bajacharaya, R.M., 2002. Land-use change in two Nepalese watersheds: GIS and geomorphometric analysis. Land Degrad. Dev. 13 (6), 495–513.

Bartlett, R., Freeman, S., Cook, J., Dongol, B.S., Sherchan, R., Shrestha, M., et al., 2011. Freshwater ecosystem vulnerability assessment: the Indrawati sub-basin, Nepal. Nicholas Institute for Environmental Policy Solutions Report, NI R 11-07, Duke University, WWF.

Bavay, M., Lehning, M., Jonas, T., Lowe, H., 2009. Simulations of future snow cover and discharge in Alpine headwater catchments. Hydrol. Process. 23, 95–108.

Betrie, G.D., Mohamed, Y.A., van Griensven, A., Srinivasan, R., 2011. Sediment management modelling in the Blue Nile Basin using SWAT model. Hydrol. Earth Syst. Sci. 15, 807–818. doi:10.5194/hess-15-807-2011.

Bhatt, D., Maskey, S., Babel, M.S., Uhlenbrook, S., Prasad, K.P., 2013. Climate trends and impacts on crop production in the Koshi River basin of Nepal. Reg. Environ. Change doi:10.1007/s10113-013-0576-6.

Bhattarai, M., Pant, D., Mishra, V.S., Devkota, H., Pun, S., Kayastha, R.N., et al., 2002. Integrated Development and Management of Water Resources for Productive and Equitable Use in the Indrawati River Basin, Nepal (Working Paper 41). International Water Management Institute (IWMI), Colombo, Sri Lanka.

Bocchiola, D., 2007. Use of Scale Recursive Estimation for multisensor rainfall assimilation: a case study using data from TRMM (PR and TMI) and NEXRAD. Adv. Water Resour. 30, 2354–2372.

Bocchiola, D., Rosso, R., 2006. The use of scale recursive estimation for short term Quantitative Precipitation Forecast. Phys. Chem. Earth 31 (18), 1228–1239.

Bocchiola, D., Diolaiuti, G., Soncini, A., Mihalcea, C., D'Agata, C., Mayer, C., et al., 2011. Prediction of future hydrological regimes in poorly gauged high altitude basins: the case study of the upper Indus, Pakistan. Hydrol. Earth Syst. Sci. 15, 2059–2075.

Bocchiola, D., Nana, E., Soncini, A., 2013. Impact of climate change scenarios on crop yield and water footprint of maize in the Po valley of Italy. Agric. Water Manage. 116, 50–61.

Brouwer, F.M., 1988. Determination of broad-scale land use changes by climate and soils. Working Paper WP-88-007, Laxenburg, Austria: International Institute for Applied Systems Analysis.

Confalonieri, R., Acutis, M., Gianni Bellocchi, G., Donatelli, M., 2009. Multi-metric evaluation of the models WARM, CropSyst and WOFOST for rice. Ecol. Modell. 220 (11), 1395–1410.

Confortola, G., Soncini, A., Bocchiola, D., 2014. Climate change will affect water resources in the Alps: a case study in Italy. J. Alp. Res. 100–103. <http://rga.revues.org/2176>.

Cook, S., Rubiano, J., Sullivan, C., Andah, W., Ashante, F., Wallace, J., et al., 2007. Waterpoverty mapping in the Volta basin, CGIAR Challenge program on water and food. Workshop report, Accra, Ghana 3–8 March. <http://cpwfbfp.pbworks.com/f/Water_poverty_mapping_Volta_Ghana_Workshop_Report.pdf>.

DHM, 2010. Department of hydrology and meteorology. Ministry of Environment Nepal.

Dijkshoorn, K., Huting, J., 2009. Soil and terrain database for Nepal (1:1 million). ISRIC World Soil Information, Report 2009/01.

Dulal, H.B., Brodnig, G., Thakur, H.K., Green-Onoriose, C., 2010. Do the poor have what they need to adapt to climate change? A case study of Nepal. Local Environ. 15 (7), 621–635.

Eriksson, M., Xu, J.C., Shrestha, A.B., Vaidya, R.A., Santosh, N., Sandström, K., 2009. The Changing Himalayas: Impact of Climate Change on Water Resources and Livelihoods in the Greater Himalayas. Publ. ICIMOD, Kathmandu. ISBN 978-92-9115-111-0.

Fader, M., Gerten, D., Thammer, M., Lotze-Campen, H., Lucht, W., Cramer, W., 2011. Internal and external green-blue agricultural water footprints of nations, and related water and land savings through trade. Hydrol. Earth Syst. Sci. 15, 1641–1660.

FAO, 2009. Adapting to climate change. In Unasylva, 60, (231/232).

Gent, P.R., Danabasoglu, G., Donner, L.J., Holland, M.M., Hunke, E.C., Jayne, S.R., et al., 2011. The community climate system model version 4. J. Clim. 24, 4973–4991.

Giorgi, F., 1990. Simulation of regional climate using a limited area model nested in a general circulation model. J. Clim. 3, 941–963.

Groppelli, B., Bocchiola, D., Rosso, R., 2011a. Spatial downscaling of precipitation from GCMs for climate change projections using random cascades: a case study in Italy. Water Resour. Res. 47, W03519. doi:10.1029/2010WR009437. Groppelli, B., Soncini, A., Bocchiola, D., Rosso, R., 2011b. Evaluation of future hydrological cycle under climate change scenarios in a mesoscale Alpine watershed of Italy. NHESS 11, 1769–1785. doi:10.5194/nhess-11-1769-2011.

Hazeleger, W., Wang, X., Severijns, C., Ştefănescu, S., Bintanja, R., Sterl, A., et al., 2011. EC-Earth V2.2: description and validation of a new seamless earth system prediction model. Clim. Dynam. 39, 2611–2629.

Houghton, J.T., Ding, Y., Griggs, D.J., Noguer, M., van der Linden, P.J., Dai, X., et al., 2001. The Scientific Basis: Contribution of Working Group I to the Third Assessment Report of the Intergovernmental Panel on Climate Change. Cambridge University Press. Climate Change.

Immerzeel, W.W., van Beek, L.P.H., Bierkens, M.F.P., 2010. Climate change will affect the Asian water towers. Science 328, 1382–1385.

IPCC, 2013. Summary for policymakers. In: Stocker, T.F., Qin, D., Plattner, G.-K., Tignor, M., Allen, S.K., Boschung, J., et al. (Eds.), Climate Change 2013: The Physical Science Basis. Contribution of Working Group I to the Fifth Assessment Report of the Intergovernmental Panel on Climate Change. Cambridge University Press, Cambridge, United Kingdom and New York, NY, USA.

Izaurralde, R.C., Williams, J.R., McGill, W.B., Rosenberg, N.J., Quiroga Jakas, M.C., 2006. Simulating soil C dynamics with EPIC: model description and testing against long-term data. Ecol. Modell. 192, 3–4, 362–384.

Jarvis, A.J., Mansfield, T.A., Davies, W.J., 1999. Stomatal behaviour, photosynthesis and transpiration under rising $CO_2$. Plant Cell Environ. 22, 639–648.

Karki, R., Gurung, A., 2012. An overview of climate change and its impact on agriculture: a review from least developing country, Nepal. Int. J. Ecosys. 2 (2), 19–24.

Karmacharya, J., Shrestha, A., Rajbhandari, R., 2007. Climate change scenarios for Nepal based on regional climate model RegCM3, Department of Hydrology and Meteorology Kathmandu – Nepal. Final report of the Project: "Enhancement of National Capacities in the Application of Simulation Models for Assessment of Climate Change and Its Impacts on Water Resources and Food and Agricultural Production".

Kaser, G., Großhauser, M., Marzeion, B., 2010. Contribution potential of glaciers to water availability in different climate regimes. PNAS 107 (47), 20223–20227. Kim, H.Y., Lieffering, M., Kobayashi, K., Okada, M., Miura, A., 2003. Seasonal changes in the effects of elevated CO2 on rice at three levels of nitrogen supply: a free air CO2 enrichment (FACE) experiment. Glob. Change Biol. 9 (6), 826–837.

Konar, M., Dalin, C., Suweis, S., Hanasaki, N., Rinaldo, A., Rodriguez Iturbe, I., 2011. Water for food: the global virtual water trade network. Water Resour. Res. 47, W05520. doi:10.1029/2010WR010307.

Konz, M., Uhlenbrook, S., Braun, L., Shrestha, A., Demuth, S., 2007. Implementation of a process-based catchment model in a poorly gauged, highly glacierized Himalayan headwater. Hydrol. Earth Syst. Sci. 11 (4), 1323–1339.

Leuning, R., 1995. A critical appraisal of a combined stomatal photosynthesis model for C3 plants. Plant Cell Environ. 18, 357–364.

Malla, G., 2008. Climate change and its impact on Nepalese agriculture. J. Agric. Environ. 9, 62–71.

Maskey, S., Uhlenbrook, S., Ojha, S., 2011. An analysis of snow cover changes in the Himalayan region using MODIS snow products and in-situ temperature data. Clim. Change 108 (1–2), 391–400.

McMurtrie, R.E., Norby, R.J., Medlyn, B.E., Dewar, R.C., Pepper, D.A., Reich, P.B., et al., 2008. Why is plant-growth response to elevated CO2 amplified when water is limiting, but reduced when nitrogen is limiting? A growth-optimisation hypothesis. Funct. Plant Biol. 35, 521–534.

Monteith, J.L., Moss, C.J., 1977. Climate and the efficiency of crop production in Britain. Phil. Trans. R. Soc. Lond. B 281, 277–294.

Morison, J.I.L., 1999. Interactions between increasing CO2 concentration and temperature on plant growth. Plant Cell Environ. 22 (6), 659–682.

Nana, E., Corbari, C., Bocchiola, D., 2014. A hydrologically based model for crop yield and water footprint assessment: study of maize in the Po valley. Agric. Syst. 127, 139–149.

NAPA, 2010. National Adaptation Programme of Action (NAPA). Government of Nepal, Ministry of Environment, Kathmandu, Nepal.

Neitsch, S.L., Arnold, J.G., Kiniry, J.R., Williams, J.R., 2011. Soil and water assessment tool. Theoretical documentation, version 2009. Texas Water Resources Institute Technical Report N°406.

Nyaupanea, G.P., Chhetrib, N., 2009. Vulnerability to climate change of nature-based tourism in the Nepalese himalayas. Tourism Geogr. 11 (1), 95–119.

Olesen, J.E., Bindi, M., 2002. Consequences of climate change for European agricultural productivity, land use and policy. Eur. J. Agron. 16, 239–262.

Olesen, J.E., Carter, T.R., Diaz-Ambrona, C.H., Fronzek, S., Heidmann, T., Hickler, T., et al., 2007. Uncertainties in projected impacts of climate change on European agriculture and terrestrial ecosystems based on scenarios from regional climate models. Clim. Change 81, 123–143.

Parry, M.L., Rosenzweig, C., Iglesias, A., Livermore, M., Fischer, G., 2004. Effects of climate change on global food production under SRES emissions and socio-economic scenarios. Global Environ. Change 14, 53–67.

Peel, M.C., Finlayson, B.L., McMahon, T.A., 2007. Updated world map of the Köppen-Geiger climate classification. Hydrol. Earth Syst. Sci. 11, 1633–1644.
Rai, M., 2007. Climate change and agriculture: a Nepalese case. J. Agric. Environ. 8, 92–95.
Rosenzweig, C., Hillel, D., 1998. Climate Change and the Global Harvest. Oxford University Press, New York.
Rost, S., Gerten, D., Bondeau, A., Lucht, W., Rohwrer, J., 2008. Agricultural green and blue water consumption and its influence on the global water system. Wat. Resour. Res. 44, W09405, 17 pp.
Rupa Kumar, K., Sahai, A.K., Krishna Kumar, K., Patwardhan, S.K., Mishra, P.K., Revadekar, J.V., et al., 2006. High resolution climate change scenario for India for the 21st century. Curr. Sci. 90 (3), 334–345.
Schuol, J., Abbaspour, K.C., Yang, H., Srinivasan, R., Zehnder, A.J.B., 2008. Modeling blue and green water availability in Africa. Water Resour. Res. 44, W07406. doi:10.1029/2007WR006609.
Shakya, M.K., 2011. Assessing water resources availability in Indrawati river basin in Nepal: application of SWAT model for hydrologic simula-tion. MSc Thesis, UNESCO-IHE (Institute for Water Education), Delft, The Netherlands.
Sharma, C., 2002. Effect of Melamchi water supply project on soil and water. 12th ISCO Conference, Beijing.
Sharma, M., Dahal, S., 2011. Assessment of impacts of climate change and local adaptation measures in agriculture sector and livelihoods of indi-genous community in high hills of Sankhuwasabha District, Rampur, Chitwan, Nepal.
Shrestha, A.B., Aryal, R., 2011. Climate change in Nepal and its impact on Himalayan glaciers. Reg. Environ. Change 11 (1), 65–77.
Sijapati, S., Maskey, S., Timilsina, U., Ezee, G.C., Acharya, S., Timilsina, B., et al., 2013. Variability of cropping system and crop production in different agro-ecological zones in the Indrawati River Basin in Nepal. Proc. International Conference on Climate Change, Water Resources and Disasters in Mountainous Regions: Building Resilience to Changing Climate. Kathmanndu, Nepal.
Soncini, A., Bocchiola, D., 2011. Assessment of future snowfall regimes within the Italian Alps using general circulation models. Cold Regions Sci. and Tech. 68 (3), 113–123.
SRTM, 2010. Shuttle Radar Topography Mission, SRTM 90 m digital elevation data. From Shuttle Radar Topography Mission. <http://srtm.csi.cgiar.org>.
Stevens, B., Giorgetta, M., Esch, M., Mauritsen, T., Crueger, T., Rast, S., et al., 2013. Atmospheric component of the MPI-M Earth System Model: ECHAM6. J. Adv. Model. Earth Syst. 5, 1–27.
Stöckle, C., Donatelli, M., Roger, N., 2003. CropSyst, a cropping systems simulation model. Eur. J. Agron. 18, 289–307.
Stöckle, C.O., Nelson, R., 1999. Cropping Systems Simulation Model User Manual. Washington State University. <http://www.sipeaa.it/tools/CropSyst/CropSyst_manual.pdf>.
Stöckle, C.O., Williams, J.R., Rosenberg, N.J., Jones, C.A., 1992. A method for estimating the direct and climatic effects of rising atmospheric carbon dioxide on growth and yield of crops: Part I. Modification of the EPIC model for climate change analysis. Agric. Syst. 38, 225–238.
Supit, I., van Diepen, C.A., de Wit, A.J.W., Kabat, P., Baruth, B., Ludwig, F., 2010. Recent changes in the climatic yield potential of various crops in Europe. Agric. Syst. 103, 683–694.
Torriani, D., Calanca, P., Lips, M., Amman, H., Beniston, M., Fuhrer, J., 2007. Regional assessment of climate change impacts on maize productivity and associated production risk in Switzerland. Reg. Environ. Change 7, 209–221.
Tubiello, F.N., Donatelli, M., Rosenzweig, C., Stockle, C., 2000. Effects of climate change and elevated CO2 on cropping systems: model predictions at two Italian sites. Eur. J. Agron. 13, 179–189.
WaterBase, 2010. WaterBase. From WaterBase projects of United Nations University: <http://www.waterbase.org>.
Winiger, M., Gumpert, M., Yamout, H., 2005. Karakoram–Hindukush–Western Himalaya: assessing high-altitude water resources. Hydrol. Process. 19, 2329–2338.
World Bank, 2012. Data bank. World development indicators. Data by country, Nepal. <http://databank.worldbank.org/data/views/reports/tableview.aspx>.
WWF, World Wildlife Fund, Nepal, 2012. Water poverty of Indrawati basin, analysis and mapping, June 2012. <http://awsassets.panda.org/downloads/water _poverty_book.pdf>.
Zanoni, F., Duce, P., 2003. Agricoltura italiana e i cambiamenti climatici [Italian agriculture and climate changes]. Atti: CLIMAGRI-Cambiamenti climatici e agricoltura, Cagliari 16–17 Gennaio 2003, 15–22.